

# 1

## Bose–Einstein condensates in neutron stars

C. J. Pethick

*The Niels Bohr International Academy, The Niels Bohr Institute,  
University of Copenhagen, Blegdamsvej 17, DK-2100 Copenhagen Ø,  
Denmark*

*NORDITA, KTH Royal Institute of Technology and Stockholm University,  
Roslagstullsbacken 23, SE-10691 Stockholm, Sweden*

Thomas Schäfer

*Department of Physics, North Carolina State University,  
Raleigh, NC 27695-8202, U.S.A.*

A. Schwenk

*Institut für Kernphysik, Technische Universität Darmstadt,  
D-64289 Darmstadt, Germany  
ExtreMe Matter Institute EMMI, GSI Helmholtzzentrum für  
Schwerionenforschung GmbH, D-64291 Darmstadt, Germany*

### Abstract

In the two decades since the appearance of the book “Bose–Einstein Condensation” in 1995, there have been a number of developments in our understanding of dense matter. After a brief overview of neutron star structure and the Bose–Einstein condensed phases that have been proposed, we describe selected topics, including neutron and proton pairing gaps, the physics of the inner crust of neutron stars, where a neutron fluid penetrates a lattice of nuclei, meson condensates, and pairing in dense quark matter. Especial emphasis is placed on basic physical effects and on connections to the physics of cold atomic gases.

### 1.1 Introduction

Neutron stars contain strongly interacting matter under extreme conditions. The high densities, up to  $\sim 10^{15} \text{ g cm}^{-3}$  in the interior, combined with the physics of the strong interaction, which involves a rich spectrum of particles and attractive interaction channels, can lead to the realisation of various condensates in neutron stars. In this chapter, we give an overview of these possibilities, ranging from pairing of nucleons, to condensates of mesons,

to quark pairing. After a description of the structure of neutron stars, we provide an introduction to the various condensates, focusing on new developments since the book “Bose-Einstein Condensation” in 1995 [1].

We first discuss superfluid phases of neutrons and protons. These are rather well established and the present challenge is to make reliable calculations of pairing gaps and critical temperatures. This area has benefited significantly from the connections to cold atomic Fermi gases with resonantly tuned strong interactions. If hyperons are present in neutron stars, additional paired phases of hyperons are possible. At asymptotically high densities, the interaction between quarks becomes weak and the pairing of quarks is well established theoretically in this limit. We discuss how the nature of the gluon-exchange interaction gives rise to special features for quark pairing. At intermediate densities, the condensation of pions and kaons is possible. Whether or not these phases exist in nature is an open question because of the difficulty of making reliable calculations of the effects of strong correlations: this is true irrespective of whether one approaches the problem from low densities, using hadron degrees of freedom, or from high densities, where quark degrees of freedom are the natural choice. Finally, we discuss briefly some observational consequences of condensation in neutron stars, including the cooling of neutron stars, the impact on rotational behaviour and on phenomena involving the neutron star crust.

## 1.2 Neutron star structure

Matter in a neutron star ranges in density from typical terrestrial values at the surface to greater than nuclear density at the centre. In all but the outermost parts of the star, the thermal energy  $k_B T$ , where  $k_B$  is the Boltzmann constant and  $T$  the temperature, is low compared with characteristic excitation energies of the system: the star is thus a low temperature system in which quantum effects play an important role. Despite their name, neutron stars contain ingredients other than neutrons. At the surface of the star, matter in its ground state consists of  ${}^{56}_{26}\text{Fe}$  nuclei, with an equal number of electrons to ensure charge neutrality: thus, in the nucleus the number of neutrons, 30, is only slightly greater than that of protons, 26. The Fermi energy of the electrons increases rapidly with depth and it becomes energetically favourable for electrons to be captured by protons, thereby producing nuclei that are more neutron-rich.<sup>1</sup>

At a density of around  $4 \times 10^{11} \text{ g cm}^{-3}$ , around one thousandth of nuclear

<sup>1</sup> For a review of the physics of the outer parts of neutron stars see [2].

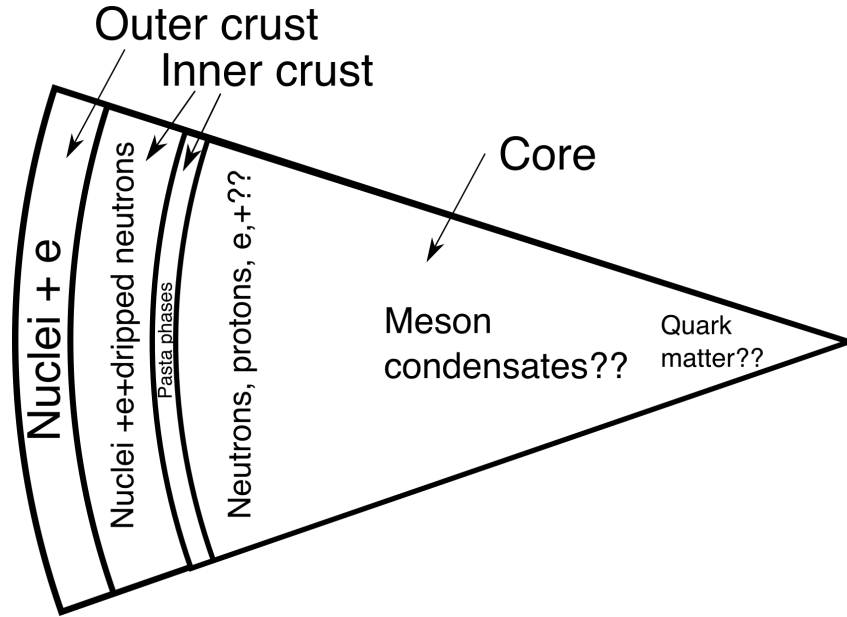


Figure 1.1 Schematic picture of the phases encountered in a neutron star.

density, the highest occupied neutron levels are no longer bound, a situation referred to as “neutron drip”. As a consequence, at higher densities the lattice of nuclei is permeated by a neutron fluid. With further increase in density, the density of this neutron fluid increases, and nuclei become even more neutron rich and occupy an increasing fraction of space. Nuclei merge to form a uniform fluid of neutrons and protons at a density of around one half of nuclear density, and the fraction of protons is  $\sim 5\%$ . At densities just below that for the transition to a uniform medium, nuclei can form highly non-spherical shapes such as rods or sheets in what are referred to as “pasta phases” because of their resemblance to spaghetti and lasagna. At higher densities other constituents can appear: among these are muons, (which are present when the electron chemical potential exceeds the muon restmass energy), hyperons and possible phases with deconfined quarks. A schematic view of a slice of a neutron star is shown in Fig. 1.1. The figure is not to scale. For neutron stars in the mass range that can be observed, the radius is  $\sim 12$  km [3], the outer crust is some hundreds of metres thick and the inner crust about one half of a kilometre.

### 1.3 Condensates in neutron stars

We now give an overview of the various condensates that have been proposed. These may be classified according to the baryon number,  $B$ , of the condensed boson.<sup>2</sup> At the lower densities encountered in the inner crust and the outer part of core of the star, condensates of neutron pairs and of proton pairs, which have  $B = 2$ , have been studied extensively. These are analogous to condensates in conventional metallic superconductors and, in the case of pairs with nonzero orbital angular momentum, the superfluid phases of liquid  $^3\text{He}$ . At supranuclear densities, condensates of pions and of kaons, which have  $B = 0$ , have been proposed. At even higher densities one expects matter to consist of deconfined quarks, and interactions between these can lead to condensates of pairs of quarks, which have  $B = 2/3$ .

#### 1.3.1 Pairing of nucleons

##### *Neutron pairing*

Even before the first identification of neutron stars in the cosmos and shortly after the formulation of the Bardeen–Cooper–Schrieffer (BCS) theory of superconductivity [4], Migdal in a side remark in a paper on superfluidity and the moment of inertia of atomic nuclei commented that, in matter in the interior of neutron stars, neutrons would pair with a transition temperature of order 1 MeV ( $10^{10}$  K) and that this would lead to interesting cosmological phenomena [5]. Estimates of transition temperatures for neutrons were made by Ginzburg and Kirzhnits [6], who also pointed out that the heat capacity of matter at temperatures significantly below the transition temperature would be reduced, thereby increasing the cooling rate of the star.

Initially, pairing in the singlet, S-wave state ( $^1\text{S}_0$ ) was considered. However, on the basis of calculations of the pairing gap which used interactions deduced from nucleon–nucleon scattering data, Hoffberg et al. showed that, at densities in excess of roughly nuclear density, pairing in a spin-triplet state with unit orbital angular momentum would lead to a lower energy [7]. Explicitly, the state was found to be  $^3\text{P}_2$ , in which the orbital and spin angular momenta are aligned.<sup>3</sup> This takes advantage of the fact that the nuclear spin–orbit interaction is attractive (in contrast to atomic physics where it is repulsive), thereby favouring parallel spin and orbital angular

<sup>2</sup> Irrespective of whether the condensed entity is a pair of fermionic excitations, as in a superconductor, or a bosonic excitation such as a meson, we shall refer to it simply as a “boson”.

<sup>3</sup> As a consequence of the tensor character of nucleon–nucleon interactions the state contains an admixture of the  $^3\text{F}_2$  state, but for simplicity we shall refer to the state as  $^3\text{P}_2$ .

momenta. The state is closely related to the superfluid states of liquid  ${}^3\text{He}$ , which also have unit orbital angular momentum, but with the important difference that for  ${}^3\text{He}$  the spin-orbit coupling is much weaker, since it is due to the dipole–dipole interaction between the nuclear magnetic moments of the atoms.

#### *Proton pairing*

In the outer core, the ratio of protons to neutrons is of order 5%. In free space the interaction of two protons is closely equal to that between two neutrons. This is due to the fact that the effects of electromagnetic interactions are small compared with the nuclear interactions, which are approximately invariant under rotations in isospin space. If the interaction between two protons in matter were the same as that in free space, this would imply that protons would be paired, with a gap that depended on the proton density in the same way as the neutron pairing gap depended on the neutron Fermi momentum. In other words, the proton gap as a function of the total mass density would have the same basic form as that for neutrons, but shifted to  $\sim 20$  times higher densities. However, this picture is oversimplified, because the interaction between two protons is modified by the presence of the much denser neutron medium. In addition, at these densities the contributions from many-body interactions are expected to be important. A reliable calculation of the proton pairing gap taking into account both these effects is an important open problem.

### **1.3.2 Meson condensates**

#### *Pion condensation*

The composition of matter in neutron stars was initially discussed in terms of models which treated the particles as being independent. In particular, Bahcall and Wolf [8] pointed out that pions would be degenerate if their density were high enough. If pions are treated as free particles, negative pions would appear in matter when the electron chemical potential became equal to the pion rest mass. A macroscopic number of pions would then appear in the lowest energy state, forming a coherent state of the pion field. Because of interactions, the picture is more complicated, as described in detail by Baym and Campbell [9]. One of the key findings is that the most energetically favourable pion state is one with nonzero momentum. This is due to the fact that the pion is a pseudoscalar Goldstone boson, and therefore the matrix element for absorption of a pion by a nucleon is proportional to  $\boldsymbol{\sigma} \cdot \mathbf{q}$ , where  $\boldsymbol{\sigma}$  is the nucleon spin operator and  $\mathbf{q}$  the pion momentum. For example, the

interaction mixes a negative pion with proton-hole–neutron-particle states, thereby decreasing the energy of the pion. Neutron and proton states with momenta differing by the pion momentum are mixed by interaction with the pion field and the elementary fermionic excitations are linear combinations of neutrons and protons. The main obstacle to making reliable predictions of the threshold density for pion condensation is that it is expected to occur at supranuclear densities, where central, tensor, and spin-orbit correlations as well as many-body forces are important.

#### *Kaon condensation*

Because the mass of the strange quark is greater than that of up and down quarks, strange particles are not present in low density matter in equilibrium. The mass of the strange quark is roughly 100 MeV, and therefore, when chemical potentials of constituents of matter (relative to their rest masses) are of order 100 MeV and greater, it is relevant to ask whether strange particles could be present. In the normal state, there is a possibility of  $\Sigma^-$  and  $\Lambda^0$  hyperons being present. Kaplan and Nelson [10] proposed that, because of the attractive interaction between kaons and nucleons predicted by chiral theories, condensates of kaons could appear in neutron stars. In Ref. [10] the calculations were made in the mean field approximation. Subsequently, it was demonstrated that correlation effects would reduce the attraction between kaons and nucleons, thereby increasing the threshold density [11]. Estimating the threshold density for kaon condensation is challenging because of the paucity of experimental information of interactions of strange particles with other particles, in addition to the difficulties described for pion condensation.

#### *Pairing of quarks*

Up to this point, we have discussed possible Bose–Einstein condensed states of dense matter on the basis of a description in terms of hadronic degrees of freedom. In the regime of very high density it is more appropriate to use a Fermi gas of quarks as a starting point [12, 13]. It is difficult to quantify the meaning of “high density” in this context. In the case of high temperature and zero baryon density, numerical simulations of QCD on a space-time lattice show that a transition from hadronic matter to a quark gluon plasma takes place at a temperature of  $T_c \simeq 170$  MeV. The transition is a smooth crossover, and the equation of state of the plasma at temperatures  $T \gtrsim 1.5T_c$  can be described in terms of quark and gluon quasiparticles. At non-zero baryon density lattice simulations cannot be carried out because of the fermion sign problem, and as a result there is no reliable information on the

phase diagram at high baryon density. Using the mean thermal momentum at  $T_c$  as a guide for the Fermi momentum in quark matter near the critical quark chemical potential we get  $\mu_c \simeq 500$  MeV, corresponding to a baryon density  $\rho \simeq 10\rho_0$ , where  $\rho_0 \approx 0.16$  fm<sup>-3</sup> is the nuclear saturation density. This is quite large, but there are indications that the transition from quark matter to nuclear matter is smooth [14], so that calculations in the high-density limit may provide useful constraints on the behaviour of matter at moderate density.

The presence of a Fermi surface combined with the attractive interaction between quarks implies that the BCS mechanism will lead to Cooper pairing and superfluidity even if the gluon-mediated interaction is weak. This was proposed by Ivanenko and Kurdgelaidze [15] even before the development of QCD. Subsequently, following the understanding of asymptotic freedom, which implies that interactions between quarks become weak at high densities, pairing between quarks of different flavours was considered in Refs. [16, 17], see [18] for a review. Interest in pairing of quarks revived about two decades ago with the appreciation that large pairing gaps can arise in states in which the flavours of quarks are correlated with their colours.

## 1.4 Recent developments

In this section we describe some of the developments during the past two decades. As we shall show, there are a number of points of contact between the physics of dense matter and that of ultracold atomic gases.

### 1.4.1 Uniform neutron matter

As described earlier, at densities above that for neutron drip, matter consists of a lattice of nuclei immersed in an electron gas with an interstitial fluid of neutrons, whose density increases from very low values just above neutron drip to ones approaching nuclear density at the inner edge of the crust. For most of this density range, the nuclei occupy a small fraction of space and to a very good approximation the neutron fluid may be treated as being homogeneous. This neutron fluid cannot be studied directly in the lab, and therefore its properties must be determined theoretically. The interaction between two neutrons in an S-wave state at low energy is described by the scattering length, which is  $a_S \approx -18.5$  fm, and by an effective range  $r_e \approx 2.7$  fm, which is relevant for the inner crust. Since the interaction is attractive, a low-density neutron gas will be paired in the  $^1S_0$  state. In what

we shall refer to as the BCS approximation, one assumes that the interaction between two neutrons is the same as the interaction in free space, and the effect of the medium on the interaction and on the single-particle properties is neglected. One then finds that the neutron pairing gap in the dilute limit is given by

$$\Delta_{\text{BCS}} = \frac{8}{e^2} E_F \exp\left(-\frac{\pi}{2k_F|a_s|}\right), \quad (1.1)$$

where  $E_F = \hbar^2 k_F^2 / 2m_n$  is the Fermi energy,  $k_F$  being the Fermi wave number and  $m_n$  the neutron mass.

It came as something of a surprise to find that this is a poor approximation even in the limit of low densities. This was well understood long ago by Gor'kov and Melik-Barkhudarov [19] in a paper that was largely unnoticed until attention was drawn to it after the experimental realisation of degenerate atomic Fermi gases [20]. They showed that in the low-density limit the gap is given by

$$\Delta = \left(\frac{2}{e}\right)^{7/3} E_F \exp\left(-\frac{\pi}{2k_F|a_s|}\right), \quad (1.2)$$

which is  $(4e)^{-1/3} \approx 0.45$  of its value in the BCS approximation. The suppression is readily understood in terms of the modification of the interaction between two neutrons by the presence of other neutrons. At the lowest densities, the excitations in the medium are particle-hole pairs, which correspond to either density fluctuations or spin fluctuations. Exchange of density fluctuations leads to an attractive interaction, as is well known in the case of conventional superconductors, where the density fluctuation is a lattice phonon. However, exchange of spin fluctuations, i.e., particle-hole pairs with spin 1, gives a repulsive interaction. For exchange of spin fluctuations with spin-projection  $m_S = 0$  the interaction between a neutron with spin up and one with spin down is positive, because the two neutrons exchanging the spin fluctuation have opposite spins and therefore couple to the spin fluctuation with opposite signs. For excitations with  $m_S = \pm 1$ , the interaction is again repulsive because, although the interaction is intrinsically attractive it corresponds to an exchange interaction in the pairing channel since it reverses the roles of the spin-up and spin-down neutrons undergoing pairing, thereby introducing an additional minus sign.

At higher densities, other many-body effects must be taken into account, and a variety of methods have been used to calculate the properties of neutron matter. The best present-day techniques are a family of Quantum Monte Carlo methods, which are accurate enough at lower densities that it is



possible to calculate pairing gaps from the differences between the energies of systems with odd and even particle numbers (For a review of these developments, see [21]). Thanks to these methods, coupled with the analytical results in the low-density limit, the neutron gap is now well understood at densities less than about one tenth of nuclear density, where the effects of the two-body interactions beyond the S-wave contribution and of three-body interactions may be neglected. The current challenge is to calculate neutron pairing gaps at higher densities, at which correlations become stronger and three-body interactions play an important role. (At saturation density, the leading four-body forces in chiral effective field theory have been shown to be very small, an order of magnitude smaller than 3N interactions.)

To calculate gaps for non-S-wave pairing is more difficult, because these depend not on the pairing interaction averaged over angles between the initial and final momenta of the fermions undergoing scattering, as in the case of S-wave pairing, but on deviations of the pairing interaction from this average value. For  ${}^3\text{P}_2$  pairing, the role of correlations, in particular from induced spin–orbit interactions, has only been explored at low order in a many-body expansion [22]; these calculations led to very small  ${}^3\text{P}_2$  gaps, but the possibilities that the  ${}^3\text{P}_2$  gap vanishes or that pairing is stronger in some other channel are not excluded.

#### 1.4.2 Superfluid neutrons in the inner crust

In the inner crust, the neutron superfluid permeates a lattice of nuclei. Low-frequency, long-wavelength phenomena may be described by a two-fluid model, the two fluids corresponding, loosely speaking, to the superfluid neutrons and the nuclei [23]. For a spatially uniform neutron fluid, at zero temperature Galilean invariance leads to the conclusion that the neutron superfluid density is equal to the total neutron density. However, for neutrons in a lattice of nuclei, the neutron superfluid density is less than the total neutron density because of what in the language of quantum liquids is referred to as “backflow” and in the neutron star literature as “entrainment”. The two terms reflect different aspects of the problem, the first emphasising the disturbance of the neutron current density caused by the nuclei, the second the fact that part of the neutron density is locked to the nuclei and does not contribute to the superfluid flow.

The neutron superfluid density is an important quantity in models of a number of phenomena observed in pulsars. One is sudden speed-ups (glitches) of the rotation frequency of the pulsar, which in some models is attributed to superfluid neutrons weakly coupled to the crust and other normal parts

of the star (for reviews of glitch phenomena see [24, 25]): here the moment of inertia of the superfluid neutrons, which is directly related to the neutron superfluid density, plays a key role (see, e.g., [26, 27]). Another is in explaining quasiperiodic oscillations observed in the X-ray afterglows of giant flares from highly magnetised neutron stars, a possible model for which is oscillations of the crust of the neutron star [28, 29]. The frequency of these modes is sensitive to the neutron superfluid density in the crust.

To the extent that the lattice is rigid, the system thus resembles a superfluid atomic Fermi gas in a three-dimensional optical lattice. An important difference, however, is that the number of neutrons per unit cell can be as high as  $\sim 10^3$ . As a consequence of the large number of neutrons per unit cell, a corresponding large number of bands in the neutron band structure must be taken into account: this represents a considerable challenge. If the effects of neutron pairing are weak, the neutron superfluid density is simply related to the response of a current in the normal state to a vector potential. Chamel has performed mean-field (Hartree–Fock) calculations of the band structure of neutrons in the normal state and finds that the neutron superfluid density can be a factor of 10 or more smaller than the density of neutrons between nuclei, which one might expect to be a reasonable first estimate of the superfluid density [30].

An important open problem is to make improved calculations of the neutron superfluid density that take into account both band structure and pairing. As an indication of the need to include both effects simultaneously, one may mention the fact that in the part of the inner crust where the neutron gap attains its largest values, the coherence length, which is the dimension of a neutron pair, is less than the lattice spacing. The corresponding problem for fermionic atoms with resonant interactions in a one-dimensional optical lattice has been addressed in Ref. [31] and recently Watanabe has extended these calculations to atoms with interactions that are not resonant [32]. What is needed is an extension of this work to three-dimensional lattices and to higher numbers of atoms per unit cell.

### *1.4.3 A dilute solution of protons in neutrons*

In the outer core of a neutron star, matter is expected to be a uniform fluid of neutrons with a  $\sim 5\%$  admixture of protons (together with an equal admixture of electrons to maintain charge neutrality). Since the protons are a minority component and the coupling of neutrons and protons is strong, interactions between protons in the medium are modified by the presence of the neutrons. Dilute mixtures of atoms have been studied extensively, as have

dilute solutions of  ${}^3\text{He}$  in liquid  ${}^4\text{He}$ , where solutions with a concentration of a few per cent have received particular attention.

To illustrate how insights from cold gases may be exploited, let us consider the interaction of two protons with opposite spins induced by the presence of the nuclear medium.<sup>4</sup> Since the neutron medium has both spin- and density degrees of freedom, the induced interaction has two contributions, one from exchange of density fluctuations (as in dilute solutions of  ${}^3\text{He}$ ) and the other from exchange of spin fluctuations (see, e.g., Ref. [35]). A new feature of the proton solutions compared with the other dilute solutions is that tensor forces are important at the relevant densities, and the theory needs to be developed to include them. In addition, the effects of three-body interactions, which are relatively unimportant in atomic gases play an important role at densities comparable to that of nuclei and above.

#### 1.4.4 Atomic analogue of pion condensation

The production of cold gases of atoms with large magnetic moments has stimulated interest in creating atomic systems in which there is a “magnetic field condensation” akin to the condensation of the pion field. In this state the atoms exhibit a static spin-density wave, which is accompanied by a spin polarisation of the nucleons. As an example, we mention the creation of cold, trapped dysprosium gases, which have magnetic moments roughly 10 times those of alkali atoms [36, 37]. Viewed from the perspective of the particles, the similarity between the two situations is clear: the dipole–dipole interaction between atoms and the one-pion-exchange (OPE) interaction between nucleons, both have a tensor structure.

An important difference between the two cases is the sign of the interaction: the electromagnetic dipole–dipole is negative for dipoles with the same orientation arranged head-to-tail, but positive for like dipoles lying side-by-side. While the tensor force between a neutron and a proton in the isospin singlet channel has the same sign as for magnetic dipoles, the opposite is the case for the spins of neutrons interacting via the one-pion-exchange interaction. For a sufficiently strong dipolar interaction, uniform matter is unstable to formation of a spin-density wave. For dipolar atoms in a one-dimensional structure, the local spin polarisation in the energetically favoured state is perpendicular to the direction of the modulation [38], while for neutrons interacting via the OPE interaction the polarisation is in the same direction as the modulation, as indicated schematically in Fig. 1.2. If the dipolar

<sup>4</sup> The analogous problem of the interaction of minority fermions in the presence of a majority fermion component has previously been considered in the context of cold atomic gases [33, 34].

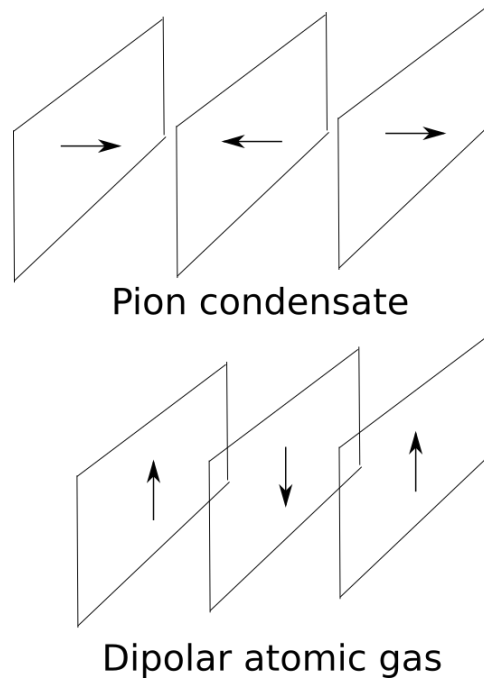


Figure 1.2 Schematic picture of the neutron spin density wave in a neutral pion condensed state (upper diagram) and in an atomic gas with dipolar interactions (lower diagram). The magnetization density is uniform on the planes indicated and varies smoothly in between. Due to nonlinear effects, the spin-density wave will be accompanied by a density wave with a wave vector equal to twice that of the spin-density wave. For this reason, the phases are referred to as “smectic” because of their resemblance to smectic liquid crystals.

interaction is weak compared with the central part of the interaction, a ferromagnetic state is predicted to be favourable.

The magnetic dipolar interaction differs from the OPE interaction in that it is long-range. As a consequence, in finite geometry, such as a trapped atomic cloud, the equilibrium state will be influenced by the energy of the

magnetic field outside the cloud. As an example, consider matter which in bulk is predicted to be ferromagnetic: in a cloud the direction of the magnetisation will vary in direction in order to reduce the magnetic field energy outside the cloud, an effect analogous to formation of domains in a solid ferromagnet. However, because of the absence of the lattice, the thickness of the domain walls is comparable to the size of a domain. Further work is required to determine in detail the structure of dipolar atomic gases, as a function of the strengths of the central and dipolar parts of the interaction, the strength of the magnetic field, and the finite extent of the atomic cloud.

#### 1.4.5 Quark matter

##### *Normal state*

Even in the normal state, quark matter is an interesting system because it is an example of a marginal Fermi liquid: the velocity of a quasiparticle with momentum  $\mathbf{p}$  close in magnitude to the Fermi momentum,  $p_F$ , tends to zero as  $p \rightarrow p_F$ , whereas in a normal Fermi liquid the velocity tends to a constant. The reason for this unusual behaviour is that, because gluons are massless, the gluon-exchange interaction is long-range. The interaction is made up of colour-electric (longitudinal) and colour-magnetic (transverse) contributions in essentially the same way as for the electric and magnetic contributions to the interaction between two electrical charges. The coupling of gluons to quarks is governed by a coupling constant  $g$  that depends on the momentum transfer. The sign of  $g$ , like that of the charge of the electron, is a matter of convention and we take it to be positive. The dimensionless quantity  $g^2/\hbar c$  is the QCD analogue of the fine structure constant  $\alpha = e^2/\hbar c$  in QED. Asymptotic freedom implies that the typical interaction between quarks decreases as the density and the Fermi momentum increase. If one neglects the effects of the medium on the gluons, the quark self energy due to emission and absorption of a gluon diverges. In a medium, the electric part of the interaction is cut off at wave numbers less than the screening wave number  $k_D \sim gp_F$  by Debye screening.<sup>5</sup> However, because quarks do not possess a magnetic frequency, magnetic fields are not screened at zero frequency, but at nonzero frequency  $\omega$ , magnetic interactions are cut off at wave numbers less than  $(g^2|\omega|p_F^2)^{1/3}$  by Landau damping. In more technical

<sup>5</sup> To avoid making formulae cumbersome, in the remainder of this section we use units in which  $c$ ,  $\hbar$  and the Boltzmann constant  $k_B$  are equal to unity.

terms, the transverse gluon propagator has the form [39]

$$D_{ij}(\omega, \mathbf{k}) = \frac{\delta_{ij} - \hat{k}_i \hat{k}_j}{\omega^2 - c^2 k^2 + i\pi k_D^2 \omega/k} \quad (1.3)$$

for  $|\omega| \leq k$ . In the physics of normal metals, the analogous phenomenon for electrodynamics is known as the anomalous skin effect: when the mean free path of an electron becomes larger than the wavelength of an applied magnetic field, the length relevant in determining the response is the wavelength rather than the mean free path.

So far we have concentrated on the interaction between quarks, and have assumed that near the Fermi surface in the normal state the spectrum is linear in  $p - p_F$ . However, from a one-loop calculation using Eq. (1.3) for the one-gluon transverse propagator one finds that the quark propagator behaves as

$$S(\nu, \vec{p}) = \frac{Z_F}{\nu - v_F(p - p_F)}, \quad (1.4)$$

with  $Z_F \sim v_F \sim [g^2 \log(k_D/|\nu|)]^{-1}$ . This implies that the quasiparticle wave function and velocity vanish on the would-be Fermi surface.<sup>6</sup> One might suspect that this breakdown of Fermi liquid theory would severely affect estimates of gaps in superfluid phases, but this turns out not to be the case, as we shall describe below.

### *Order parameter*

We turn now to the pairing interaction between quarks. Since quarks are nearly massless the system is relativistic and  $p_F \simeq \mu_q$ , where  $\mu_q \simeq \mu_B/3$  is the quark chemical potential and  $\mu_B$  the baryon chemical potential. In relativistic theory, fermions of a particular species are described by four-component (Dirac) fields rather than the two-component spinors corresponding to the two spin components in nonrelativistic theory. The fields describing quarks,  $q_{\alpha f}^a$ , are thus labelled by a Dirac index  $\alpha$ , in addition to a colour index  $a$  (red, blue, or green) and a flavour index  $f$  (up, down, or strange).<sup>7</sup> The interaction between quarks is mediated by gluon fields  $A_\mu^c$ , which couple to the colour charges of the quarks. Here,  $c = 1, \dots, 8$  labels traceless hermitean  $3 \times 3$  matrices that act on the colour indices of the quarks. The one-gluon exchange interaction is attractive in the colour-antisymmetric

<sup>6</sup> The analogous effect for the electron gas, in that case due to exchange of transverse *photons*, was investigated long ago in Ref. [40]. However, in a nonrelativistic electron gas, the effects of transverse photons are of order  $v_F^2/c^2$  smaller than those due to the Coulomb interaction and are not observable experimentally.

<sup>7</sup> Quarks of other flavours have much higher masses and would appear only at densities considerably higher than those anticipated to occur in neutron stars.

quark–quark channel, and therefore, on the basis of the analogy with the nonrelativistic problem, one would expect quark matter to be unstable to formation of a state with quark pairs (diquarks). These pairs may be viewed as building blocks in the formation of baryons: diquarks  $D_a = \epsilon_{abc}q^bq^c$  can bind with quarks  $q^a$  to form colour neutral baryons  $B = D_aq^a$ .

The order parameter is of the form

$$\langle q_{\alpha f}^a (C\Gamma)^{\alpha\beta} q_{\beta g}^b \rangle = \phi_{fg}^{ab}, \quad (1.5)$$

where  $C$  is the charge conjugation matrix and  $\Gamma$  is a Dirac matrix.<sup>8</sup> There are many possible channels, and the ground state will depend on the flavour composition and the strength of the interaction. At very high density matter is approximately flavour symmetric, and asymptotic freedom implies that the ground state can be determined in weak coupling QCD. One finds [41, 42]

$$\langle q_{\alpha f}^a (C\gamma_5)^{\alpha\beta} q_{\beta g}^b \rangle = \phi \left( \delta_f^a \delta_g^b - \delta_g^a \delta_f^b \right), \quad (1.6)$$

which is called the colour–flavour locked (CFL) state.<sup>9</sup> The order parameter is antisymmetric in colour, as required by the interaction, and antisymmetric in both flavour and spin. This implies that the quark pairs form spin singlets. As the density is lowered, the larger mass of the strange quark becomes more important, flavour symmetry is broken, and states with a smaller spin–flavour symmetry may appear.

The colour–flavour locked state spontaneously breaks the chiral symmetry of the QCD Lagrangian, and exhibits low-energy excitations with the quantum numbers of pions and kaons. This can be seen as follows: The relation  $C\gamma_5 = C(P_L - P_R)$ , where  $P_{L,R}$  are projectors on left- and right-handedness, implies a fixed phase relation between the left- and right-handed components of the diquark condensate. The colour and flavour orientations of these condensates can be characterized by the matrices

$$X_f^a = \epsilon^{abc} \epsilon_{fgh} \langle (q_L)_g^b (q_L)_h^c \rangle, \quad Y_f^a = \epsilon^{abc} \epsilon_{fgh} \langle (q_R)_g^b (q_R)_h^c \rangle, \quad (1.7)$$

where the  $\epsilon$ -tensors take into account the antisymmetry of the CFL state under exchange of colour and of flavour. The quantities  $X_f^a$  and  $Y_f^a$  depend on the gauge choice but one can define a gauge invariant order parameter for chiral symmetry breaking by the relation  $\Sigma_f^g = X_f^a (Y^\dagger)^g_a$ .

<sup>8</sup> This expression may be regarded as the generalisation to relativistic particles of the Nambu formalism for superconductivity. There one works with (two-component) Pauli spinors and the order parameter is given in terms of spinor field operators  $\psi_\sigma$  by  $\langle \psi_\sigma \sigma_i \psi_{\sigma'} \rangle$ , where  $\sigma_i$  is a Pauli matrix. For example, with  $\Gamma = \gamma_5$  the order parameter (1.5) corresponds to the relativistic way of writing down singlet pairs, since the non-relativistic limit of  $C\gamma_5$  is  $\sigma_2$ .

<sup>9</sup> This is the simplest choice for the order parameter and corresponds to a particular gauge choice. A more general form may be obtained by performing a unitary transformation of the colour variables, which will leave unaltered variables that can be measured experimentally.

The CFL ground state corresponds to  $\Sigma \sim \mathbf{1}$ , and low energy modes with the quantum numbers of pions and kaons are described by oscillations of  $\Sigma$  in the pion direction,  $\Sigma \sim \lambda^{1,2,3}$ , or the kaon direction,  $\Sigma \sim \lambda^{4-7}$ . Here  $\lambda^a$  are the Gell-Mann matrices, a generalisation of the isospin matrices to flavour  $SU(3)$ .

In response to quark masses and lepton chemical potentials the CFL ground state can become polarised in the pion or kaon directions in flavour space. A non-zero strange quark mass, for example, favours a ground state in which there are fewer strange quarks than up and down quarks. This can be realized by a neutral kaon condensate  $\Sigma \sim \exp(i\alpha\lambda^6)$  [43]. This is a homogeneous condensate, analogous to the kaon condensate discussed from the point of view of hadronic matter in Sec. 1.3.2. For larger strange quark masses or lower densities, interactions between kaons and gapless fermion modes can lead to the formation of a standing wave kaon condensate [44]. This phase is analogous to the pion condensed state discussed above, and to standing wave ground states in Bose–Einstein condensed atomic gases, see [45, 46]. Fermion quasiparticles in these systems are quarks surrounded by a diquark polarization cloud [47], similar to the state  $B = D_a q^a$  described above. As the strength of the interaction increases, these states can continuously evolve into tightly bound baryons. A similar crossover can be studied in cold atomic gases of three fermionic species [48].

### Gaps

Superfluid gaps in quark matter have a very different dependence on coupling compared with dilute atomic gases. Since the gluon exchange interaction is of order  $g^2$ , on the basis of the calculations for a dilute atomic gas, Eq. (1.2), one might have expected  $\Delta \sim \mu_q e^{-\text{const.}/g^2}$ . In fact, for weak coupling one finds [49, 50, 51, 52, 42]

$$\Delta \simeq C_1 \frac{\mu_q}{g^5} \exp(-C_2/g), \quad (1.8)$$

where

$$C_1 = \frac{512\pi^4}{2^{1/3}} \left(\frac{2}{3}\right)^{5/2} e^{-(\pi^2+4)/8}, \quad \text{and} \quad C_2 = \frac{3\pi^2}{\sqrt{2}}. \quad (1.9)$$

The reason for the difference lies in the long-range character of the gluon exchange interaction, as discussed above. Transverse gluons do not upset the basic mechanism of the BCS instability, but they do modify the magnitude of the gap. The gap equation has two logarithmic infrared divergences, one related to the BCS mechanism and one caused by the unscreened transverse gluon exchange. The coefficient of the  $1/g$  term in the exponent is determined



by transverse gluon exchange, and the exponential term in  $C_1$  is related to the wave function renormalisation  $Z_F$  discussed above. As one sees, the fact that, in the normal state, quark matter is a marginal Fermi liquid has only a modest effect on the gap. The pre-exponential factor is set by electric gluon exchanges, and is sensitive to the symmetries of the order parameter. For  $\mu_q \simeq 500$  MeV the gap is of order 10–20 MeV.

### *Superfluidity and superconductivity*

In the CFL phase, the densities of u-, s-, and d quarks are equal and, consequently, in bulk matter there is no need for other particles, such as electrons, to ensure electrical neutrality. The CFL phase is a superfluid but an electrical insulator. Heuristically, this may be understood as being a consequence of the fact that the sum of the charges of the three flavours of quarks vanishes.<sup>10</sup>

When the flavour symmetry is broken, the net charge density of the quarks is nonzero, and this is compensated by a background of electrons. In this case, matter becomes a charged superfluid, and is an electrical superconductor.

## 1.5 Observational considerations

We now comment briefly on some observational consequences of Bose–Einstein condensation in neutron stars. Models of glitches and X-ray flares that involve superfluid flow have been mentioned in Sec.1.4.2. A more extensive account of observational effects may be found in Ref. [53].

### *1.5.1 Neutron star structure*

The mass–radius relation for neutron stars depends on the equation of state of matter, which is affected by Bose–Einstein condensation. In the case of pairing of nucleons and quarks, the predicted gaps are small compared with Fermi energies and, consequently, pairing has only a small effect on structure. For meson condensates, the picture could be very different because, if it were energetically favourable to create a pion or kaon condensate is, the energy would be reduced compared with that of the system with no condensate, and matter will become softer. This would lead to a lower maximum mass of a neutron star. The observation within the past few years of two neutron stars with masses approximately twice that of the sun with small error bars

<sup>10</sup> This argument is an oversimplification, as is explained in [18, Sec. II A.3].

[54, 55] is most simply understood in terms of an equation of state that is similar to what is expected for models based on nucleon degrees of freedom, without significant softening due to formation of a meson condensate.

### *1.5.2 Neutron star cooling*

For the first  $10^5$ - $10^6$  years after formation, a neutron star cools primarily by neutrino emission from its core. In favourable cases, emission of X-rays from the surface of the star can be detected, and the temperature of the core deduced. Since the rate of neutrino emission in dense matter depends on the microscopic properties of the matter, observations of cooling therefore have potential for providing information about the stellar interior (for a review see [56]). The path from the microscopic properties of dense matter to observed cooling curves has many steps, but the past two decades have seen a steady increase in sophistication of the modelling and the precision of observations.

As an illustration of the potential such observations have for pinning down the properties of dense matter we give a recent example. Pairing of nucleons reduces neutrino emission rates at temperatures well below the transition temperature because of the reduction in the number of thermal excitations. However, just below the transition temperature, emission of neutrino–antineutrino pairs can occur by annihilation of two thermal excitations in the superfluid. In the normal state the process is forbidden by conservation of baryon number but in the superfluid, excitations are linear combinations of normal-state particles and holes and the process is allowed. This process leads to accelerated cooling for a limited temperature range. The reported detection of changes over a period of 10 years in the surface temperature of the neutron star produced in the Cassiopeia A supernova approximately 330 years ago has been interpreted as being due to neutrons in the core undergoing a transition to a state with  $^3\text{P}_2$  pairing [57, 58]. While the analysis of the observations has been called into question, this case brings out the promise that such observations have for shedding light on pairing in neutron star cores.

## **1.6 Concluding remarks**

The study of dense matter in neutron stars has profited from work on terrestrial quantum liquids and ultracold gases. In addition, the studies of dense matter have provided inspiration for experiments in the laboratory. In the future one may expect this synergy to continue.

Within the next few years one may expect significant improvements in calculations of properties of matter at densities of order nuclear matter density by the application of chiral effective field theories [59]. Chiral effective field theory, which incorporates the symmetries of quantum chromodynamics, provides a systematic framework for treating interactions between nucleons and, when extended to strange particles, hyperons. Using a momentum expansion scheme, the theory includes the long-range interactions due to the exchange of pions (and kaons) explicitly and general contact interactions for the shorter-range parts. Moreover, it makes predictions for consistent three- and higher-body interactions.

There are also aspects of superfluidity in neutron stars that are relatively little studied, among which one may mention superconductivity of protons in the pasta phases. The appreciation of the fact that defects can occur in these phases and thereby lead to multiply connected structures [60] implies that the proton superfluid may exhibit topologically nontrivial structures (flux lines) that are trapped by the defects.

## 1.7 Acknowledgments

We are grateful to Dmitry Kobayakov for helpful conversations and to Genaro Watanabe for communicating to us his results for the superfluid density of an atomic Fermi gas in a one-dimensional optical lattice. This work was supported in part by the NewCompStar network, COST Action MP1304, the US Department of Energy grant DE-FG02-03ER41260, and by the ERC Grant No. 307986 STRONGINT.

## References

- [1] Griffin, A., Snoke, D. W., and Stringari, S. (eds). 1995. *Bose–Einstein Condensation*. Cambridge: Cambridge University Press.
- [2] Pethick, C. J., and Ravenhall, D. G. 1995. Matter at large neutron excess and the physics of neutron star crusts. *Annu. Rev. Nucl. Part. Sci.*, **45**, 429–484.
- [3] Hebeler, K., Lattimer, J. M., Pethick, C. J., and Schwenk, A. 2013. Equation of state and neutron star properties constrained by nuclear physics and observation. *Ap. J.*, **773**, 11.
- [4] Bardeen, J., Cooper, L. N., and Schrieffer, J. R. 1957. Theory of superconductivity. *Phys. Rev.*, **108**, 1175–1204.
- [5] Migdal, A. B. 1960. Superfluidity and the moments of inertia of nuclei. *Sov. Phys. JETP*, **10**, 176.
- [6] Ginzburg, V. L., and Kirzhnits, D. A. 1965. On the superfluidity of neutron stars. *Sov. Phys. JETP*, **20**, 1346–1348.

- [7] Hoffberg, M., Glassgold, A. E., Richardson, R. W., and Ruderman, M. 1970. Anisotropic superfluidity in neutron star matter. *Phys. Rev. Lett.*, **24**, 775–777.
- [8] Bahcall, J. N., and Wolf, R. A. 1965. Neutron stars. I. Properties at absolute zero temperature. *Phys. Rev.*, **140**, B1445–1451.
- [9] Baym, G., and Campbell, D. K. 1978. Chiral symmetry and pion condensation. Pages 1031–1094 of: Rho, M., and Wilkinson, D. H. (eds), *Mesons in Nuclei*, vol. III. Amsterdam: North Holland.
- [10] Kaplan, D. B., and Nelson, A. E. 1986. Strange goings on in dense nucleonic matter. *Phys. Lett. B*, **175**, 57–63.
- [11] Pandharipande, V. R., Pethick, C. J., and Thorsson, V. 1995. Kaon energies in dense matter. *Phys. Rev. Lett.*, **75**, 4567–4570.
- [12] Collins, J. C., and Perry, M. J. 1975. Superdense matter: Neutrons or asymptotically free quarks? *Phys. Rev. Lett.*, **34**, 1353–1356.
- [13] Baym, G., and Chin, S. A. 1976. Can a neutron star be a giant MIT bag? *Phys. Lett. B*, **62**, 241–244.
- [14] Schäfer, T., and Wilczek, F. 1999. Continuity of quark and hadron matter. *Phys. Rev. Lett.*, **82**, 3956–3959.
- [15] Ivanenko, D., and Kurdgelaidze, D. F. 1969. Remarks on quark stars. *Nuovo Cim. Lett.*, **2**, 13–16.
- [16] Barrois, B. C. 1977. Superconducting quark matter. *Nucl. Phys. B*, **129**, 390–396.
- [17] Bailin, D., and Love, A. 1979. Superfluid quark matter. *J. Phys. A Math. Gen.*, **12**, L283–L289.
- [18] Alford, M. G., Schmitt, A., Rajagopal, K., and Schäfer, T. 2008. Color superconductivity in dense quark matter. *Rev. Mod. Phys.*, **80**, 1455–1515.
- [19] Gor'kov, L. P., and Melik-Barkhudarov, T. K. 1961. Contribution to the theory of superfluidity in an imperfect Fermi gas. *Sov. Phys. JETP*, **13**, 1018–1022.
- [20] Heiselberg, H., Pethick, C. J., Smith, H., and Viverit, L. 2000. Influence of induced interactions on the superfluid transition in dilute Fermi gases. *Phys. Rev. Lett.*, **85**, 2418–2421.
- [21] Gezerlis, A., Pethick, C. J., and Schwenk, A. 2014. Pairing and superfluidity of nucleons in neutron stars. Pages 580–615 of: Bennemann, K. H., and Ketterson, J. B. (eds), *Novel Superfluids*, vol. 2. Oxford: Oxford University Press.
- [22] Schwenk, A., and Friman, B. 2004. Polarization contributions to the spin-dependence of the effective interaction in neutron matter. *Phys. Rev. Lett.*, **92**, 082501.
- [23] Pethick, C. J., Chamel, N., and Reddy, S. 2010. Superfluid dynamics in neutron star crusts. *Prog. Theor. Phys. Suppl.*, **186**, 9–16.
- [24] Haskell, B., and Melatos, A. 2015. Models of pulsar glitches. *Int. J. Mod. Phys. D*, **24**, 1530008.
- [25] Link, B. in preparation.
- [26] Andersson, N., Glampedakis, K., Ho, W. C. G., and Espinoza, C. M. 2012. Pulsar glitches: The crust is not enough. *Phys. Rev. Lett.*, **109**, 241103.
- [27] Chamel, N. 2013. Crustal entrainment and pulsar glitches. *Phys. Rev. Lett.*, **110**, 011101.
- [28] Duncan, R. C. 1998. Global seismic oscillations in soft gamma repeaters. *Ap. J. Lett.*, **498**, L45–L49.
- [29] Steiner, A. W., and Watts, A. L. 2009. Constraints on neutron star crusts from oscillations in giant flares. *Phys. Rev. Lett.*, **103**, 181101.

- [30] Chamel, N. 2012. Neutron conduction in the inner crust of a neutron star in the framework of the band theory of solids. *Phys. Rev. C*, **85**, 035801.
- [31] Watanabe, G., Orso, G., Dalfovo, F., Pitaevskii, L. P., and Stringari, S. 2008. Equation of state and effective mass of the unitary Fermi gas in a one-dimensional periodic potential. *Phys. Rev. A*, **78**, 063619.
- [32] Watanabe, G. private communication.
- [33] Mora, C., and Chevy, F. 2010. Normal phase of an imbalanced Fermi gas. *Phys. Rev. Lett.*, **104**, 230402.
- [34] Yu, Z., Zöllner, S., and Pethick, C. J. 2010. Comment on “Normal phase of an imbalanced Fermi gas”. *Phys. Rev. Lett.*, **105**, 188901.
- [35] Baldo, M., and Schulze, H.-J. 2007. Proton pairing in neutron stars. *Phys. Rev. C*, **75**, 025802.
- [36] Lu, M., Youn, S. H., and Lev, B. L. 2010. Trapping ultracold dysprosium: A highly magnetic gas for dipolar physics. *Phys. Rev. Lett.*, **104**, 063001.
- [37] Lu, M., Burdick, N. Q., and Lev, B. L. 2012. Quantum degenerate dipolar Fermi gas. *Phys. Rev. Lett.*, **108**, 215301.
- [38] Maeda, K., Hatsuda, T., and Baym, G. 2013. Antiferromagnetic ground state of two-component dipolar Fermi gases: An analog of meson condensation in nuclear matter. *Phys. Rev. A*, **87**, 021604.
- [39] Baym, G., Monien, H., Pethick, C. J., and Ravenhall, D. G. 1990. Transverse interactions and transport in relativistic quark-gluon and electromagnetic plasmas. *Phys. Rev. Lett.*, **64**, 1867–1870.
- [40] Holstein, T., Norton, R. E., and Pincus, P. 1973. de Haas-van Alphen effect and the specific heat of an electron gas. *Phys. Rev. B*, **8**, 2649–2656.
- [41] Alford, M. G., Rajagopal, K., and Wilczek, F. 1999. Color flavor locking and chiral symmetry breaking in high density QCD. *Nucl. Phys. B*, **537**, 443–458.
- [42] Schäfer, T. 2000. Patterns of symmetry breaking in QCD at high baryon density. *Nucl. Phys. B*, **575**, 269–284.
- [43] Bedaque, P. F., and Schäfer, T. 2002. High-density quark matter under stress. *Nucl. Phys. A*, **697**, 802–822.
- [44] Schäfer, T. 2006. Meson supercurrent state in high-density QCD. *Phys. Rev. Lett.*, **96**, 012305.
- [45] Son, D. T., and Stephanov, M. A. 2006. Phase diagram of cold polarized Fermi gas. *Phys. Rev. A*, **74**, 013614.
- [46] Radzihovsky, L., and Sheehy, D. E. 2010. Imbalanced Feshbach-resonant Fermi gases. *Rep. Prog. Phys.*, **73**, 076501.
- [47] Kryjevski, A., and Schäfer, T. 2005. An effective theory for baryons in the CFL phase. *Phys. Lett. B*, **606**, 52–58.
- [48] Rapp, R., Zarand, G., Honerkamp, C., and Hofstetter, W. 2007. Color superfluidity and “baryon” formation in ultracold fermions. *Phys. Rev. Lett.*, **98**, 160405.
- [49] Son, D. T. 1999. Superconductivity by long-range color magnetic interaction in high-density quark matter. *Phys. Rev. D*, **59**, 094019.
- [50] Schäfer, T., and Wilczek, F. 1999. Superconductivity from perturbative one-gluon exchange in high density quark matter. *Phys. Rev. D*, **60**, 114033.
- [51] Pisarski, R. D., and Rischke, D. H. 2000. Color superconductivity in weak coupling. *Phys. Rev. D*, **61**, 074017.
- [52] Brown, W. E., Liu, J. T., and Ren, H.-c. 2000. Perturbative nature of color superconductivity. *Phys. Rev. D*, **61**, 114012.

- [53] Page, D., Lattimer, J. M., Prakash, M., and Steiner, A. W. 2014. Stellar superfluids. Pages 505–579 of: Bennemann, K. H., and Ketterson, J. B. (eds), *Novel Superfluids*, vol. 2. Oxford: Oxford University Press.
- [54] Demorest, P. B., Pennucci, T., Ransom, S. M., Roberts, M. S. E., and Hessels, J. W. T. 2010. A two-solar-mass neutron star measured using Shapiro delay. *Nature*, **467**, 1081–1083.
- [55] Antoniadis, J., Freire, P. C. C., Wex, N., Tauris, T. M., Lynch, R. S., van Kerkwijk, M. H., Kramer, M., Bassa, C., Dhillon, Vik, S., Driebe, T., Hessels, J. W. T., Kaspi, V. M., Kondratiev, V. I., Langer, N., Marsh, T. R., McLaughlin, M. A., Pennucci, T. T., Ransom, S. M., Stairs, I. H., van Leeuwen, J., Verbiest, J. P. W., and Whelan, D. G. 2013. A massive pulsar in a compact relativistic binary. *Science*, **340**, 1233232.
- [56] Yakovlev, D. G., and Pethick, C. J. 2004. Neutron star cooling. *Annu. Rev. Astron. Astrophys.*, **42**, 169–210.
- [57] Page, D., Prakash, M., Lattimer, J. M., and Steiner, A. W. 2011. Rapid cooling of the neutron star in Cassiopeia A triggered by neutron superfluidity in dense matter. *Phys. Rev. Lett.*, **106**, 081101.
- [58] Shternin, P. S., Yakovlev, D. G., Heinke, C. O., Ho, W. C. G., and Patnaude, D. J. 2011. Cooling neutron star in the Cassiopeia A supernova remnant: Evidence for superfluidity in the core. *Mon. Not. Roy. Astron. Soc.*, L108–L112.
- [59] Epelbaum, E., Hammer, H.-W., and Meissner, U.-G. 2009. Modern theory of nuclear forces. *Rev. Mod. Phys.*, **81**, 1773–1825.
- [60] Schneider, A. S., Berry, D. K., Briggs, C. M., Caplan, M. E., and Horowitz, C. J. 2014. Nuclear “waffles”. *Phys. Rev. C*, **90**, 055805.